

Polyethylene Glycols Stimulate Ca^{2+} Signaling, Cytokine Production, and the Formation of Neutrophil Extracellular Traps

Alicja Hinz¹, Sylwia Stankiewicz^{1,2}, Jacek Jakub Litewka^{2,3}, Paweł E Ferdek³, Maja Sochalska⁴, Monika Bzowska¹

¹Department of Cell Biochemistry, Faculty of Biochemistry, Biophysics and Biotechnology, Jagiellonian University, Kraków, Poland; ²Doctoral School of Exact and Natural Sciences Jagiellonian University, Kraków, Poland; ³Department of Cell Biology, Faculty of Biochemistry, Biophysics and Biotechnology, Jagiellonian University, Kraków, Poland; ⁴Department of Microbiology, Faculty of Biochemistry, Biophysics and Biotechnology, Jagiellonian University, Kraków, Poland

Correspondence: Monika Bzowska, Email monika.bzowska@uj.edu.pl

Purpose: Given the increased use of polyethylene glycol (PEG) in refining the therapeutic activity of medicines, our research focuses on explaining the potential mechanism of immune reactions associated with this polymer. We aim to investigate the interaction of different types of PEG with mouse and human immune cells, thereby contributing to understanding PEG interactions with the immune system and verifying the proinflammatory activity of the tested polymers.

Patients and Methods: Mouse macrophage and neutrophil cell lines, human peripheral blood mononuclear cells, and polymorphonuclear cells isolated from healthy donors were exposed to various PEGs. ROS, NO, and cytokine production were analyzed using fluorescence intensity, absorbance, or cytometric measurements. Toll-like receptor (TLR) signaling was verified using HEK-blue-reporter cell lines. Finally, neutrophil trap formation was studied using immunofluorescence labeling, and calcium imaging was performed using a Ca^{2+} -sensitive indicator and fluorescence microscope.

Results: Our findings show that specific PEG and mPEG are not toxic to tested mouse and human cells. However, they exert proinflammatory activity against human immune cells, as evidenced by the increased secretion of proinflammatory cytokines, such as IFN- α 2, IFN- γ , TNF- α , MCP-1, IL-8, IL-17A, and IL-23. This phenomenon is independent of PEG signaling via TLR. Additionally, mPEG10 induced the formation of neutrophil extracellular traps and intracellular calcium signaling.

Conclusion: Our finding suggests that some PEG types have proinflammatory activity against human immune cells, manifesting in the upregulated production of cytokines and neutrophils trap releasing.

Keywords: drug delivery, immunomodulation, in vitro nanotoxicity, nanoparticle functionalization, PEGylated therapeutics

Introduction

Polyethylene glycol (PEG), a hydrophilic polymer, is pivotal across various medical, pharmacy, and science applications. It is used to modify small-molecule drugs, proteins, and nanomaterials, enhancing their bioavailability, pharmacokinetics, and effectiveness. PEG ensures hydrophilicity, modulates interaction with plasma and cellular proteins, and lowers the antigenicity and immunogenicity of non-human therapeutic proteins.^{1,2} The application of PEG for drug modification has revolutionized the treatment of numerous diseases, including various therapeutics such as anticancer agents.³ Furthermore, the delivery of mRNA coding for the coronavirus Spike protein, a crucial component of Pfizer/BioNTech (BNT162b2) and Moderna vaccines, would not be possible without PEGylated lipid nanoparticles.⁴⁻⁶ These examples underscore the widespread use of PEG, making it a topic of significant interest and importance. At the same time, the increasing use of PEGylated nanopharmaceuticals translates into the occurrence of side effects in a growing number of patients.

For many years, almost all PEGylated agents were administered predominantly subcutaneously, intramuscularly, topically, or orally, and patients were not reporting any toxicity.⁷ Therefore, PEG was considered inert and safe regardless of the route of

administration.¹ However, safety concerns have been raised after dangerous side effects occurred in patients after intravenous administration of PEG-modified liposomes delivering doxorubicin (Doxil).⁸ Incidents of the acute reaction were observed immediately after Doxil injection, and this phenomenon probably resulted from the presence of PEG on the surface of liposomes. The mechanism of PEG-mediated side effects is still not fully understood, although it might be related to undesired stimulation of immune response involving complement activation.^{1,9,10} According to the existing data, Doxil may induce hypersensitivity reactions or an infusion reaction, referred to as complement activation-related pseudoallergy (CARPA), a non-IgE-mediated pseudoallergy caused by the activation of the complement system.¹¹ Several studies confirmed the role of complement activation in anaphylactic reactions observed in 25–45% of patients treated with Doxil upon the first injection.^{12–15} PEG hypersensitivity incidents involving urticaria or even anaphylactic shock are not the only alarming symptoms suggesting potential PEG toxicity. A specific response develops after administering PEGylated ovalbumin to rats or rabbits, producing anti-PEG antibodies.^{16,17} Large-scale coronavirus vaccinations have shown that Pfizer/BioNtech and Moderna vaccines also caused severe anaphylaxis in some patients. PEG is implicated in these incidents, but the immunopathogenesis and pathophysiology of this life-threatening condition have not yet been fully explained.^{6,18–20}

Most studies have focused exclusively on elucidating the immediate effects following the intravenous administration of PEGylated drugs, including testing for complement activation or anti-PEG antibodies.^{21,22} It remains unclear whether and how PEGylated nanomedicines or free PEG activate specific subtypes of immune cells. Our team has been researching the use of polyelectrolyte nanocapsules for drug delivery. Investigating the short- and long-term effects of PEGylated nanocapsules *in vivo*, we found that PEGylated nanocapsules, unlike their unmodified counterparts, affected the immune system in a way that differs from what was previously described. We observed an increase in the plasma level of several cytokines following the intravenous administration of PEGylated nanocapsules, and this effect persisted for at least two months after the last injection.²³

In this study, we set out to analyze the interaction between mouse or human immune cells and PEG differing in molecular weights in kDa (PEG2, PEG6, PEG10) and chemical structure (methoxy PEG: mPEG2, mPEG 5, mPEG 10, mPEG 20). This research holds high importance as numerous variants of this polymer find applications in nanomedicine, but the nature of their interactions with immune cells is still largely uncharted territory. We observed that particular PEGs, commonly used in this field, exhibit proinflammatory activity against human immune cells, resulting in increased secretion of specific cytokines or chemokines. Importantly, this phenomenon does not originate from PEG signaling through TLR2/1, TLR2/6, TLR4, or TLR5 receptors, which, in principle, could recognize this polymer as a ligand. Furthermore, although none of the PEG tested increased intracellular production of reactive oxygen species (ROS), mPEG10 triggered Ca²⁺ signals in freshly isolated human neutrophils and neutrophil extracellular traps (NET) formation. These findings shed new light on the potential mechanisms behind the side effects of PEG and underscore the necessity for further research to understand PEG's immunological effects in nanomedicine entirely.

Materials

Polyethylene glycols (the numbers refer to the molecular weight of specific PEG in kDa): PEG 2, PEG 6, PEG 10 or methoxy polyethylene glycols: mPEG 2, mPEG 5, mPEG 10, mPEG 20 were from Merck (Darmstadt, Germany). Cell culture agents: Dulbecco's modified Eagle's medium (DMEM) GlutaMAXTM containing 4.5 g/L or 1 g/L glucose, DMEM without phenol red containing 4.5 g/L or 1 g/L glucose, Opti-MEM, fetal bovine serum (FBS), antibiotics Penicillin-Streptomycin (10,000 U/mL penicillin and 10,000 µg/mL), and GlutaMAXTM Supplement were purchased from GIBCO (Paisley, UK). Park Memorial Institute (RPMI-1640) medium was from Lonza (Basel, Switzerland), and trypsin and sterile PBS were brought in Biowest (Nuaille, France). Dichloro-dihydro-fluorescein diacetate (DCF), dihydrorhodamine (DHR), β-mercaptoethanol and β-estradiol were from Merck (Darmstadt, Germany).

Methods

Preparation of PEG Solutions and Examination of Endotoxin Contamination

All polyethylene glycol solutions were dissolved at 50 mg/mL in sterile PBS. After PEG reconstitution, lipopolysaccharide (LPS) concentration was measured using Pierce Chromogenic Endotoxin Quant Kit (ThermoFisher Scientific, Rochester, NY,

USA) according to the manufacturer's procedure. High Standards (0.1–1.0 EU/mL) were used for standard curve preparation, and PEG or mPEG solutions were diluted ten times. The absorbance was measured at 405 nm using a microplate reader, Synergy H1 hybrid plate reader and Gene5 version 2.00.18 software (BIOTEK Instruments, Winooski, VT, USA). All tested PEG and mPEG solutions contained <0.1 EU/mL LPS.

Cells Used in Experiments and Cell Culture Conditions

Monocyte/Macrophage Cell Lines

Mouse monocyte/macrophage RAW 264.7 cells (ATCC TIB-71) and P388D1 cells (ATCC CCL-46) were obtained from the American Type Culture Collection (Manassas, VA, USA). Cells were grown in DMEM GlutaMAXTM containing 4.5 g/L with 10% (v/v) FBS.

The Estrogen-Regulated Cell Line of Mouse Neutrophil Progenitors

The estrogen-regulated mouse cell lines of neutrophil progenitors were obtained by HoxB8 retroviral transduction of wild-type bone marrow as described before. As described before, the estrogen-regulated mouse cell line of neutrophil progenitors was obtained by HoxB8 retroviral transduction of wild-type bone marrow.²⁴ As previously published, progenitors were cultured in a medium supplemented with 1 μ M β -estradiol and 1% (v/v) supernatant from Stem Cell Factor producing Chinese hamster ovary (CHO) cells.²⁵ Progenitor cells were differentiated for four days in the medium without β -estradiol. Subsequently, neutrophils (mPN) were harvested and counted.

Human Hepatocytes Model

Human hepatoma-derived HepG2 cell line (ATCC HB-8065) were obtained from the American Type Culture Collection (Manassas, VA, USA). Cells were grown in DMEM GlutaMAXTM containing 1 g/L with 10% (v/v) FBS.

Human Immune Cells Isolated from the Blood

Human peripheral blood mononuclear cells (hPBMC) and human polymorphonuclear neutrophils (hPMN) were isolated from the citrated blood of healthy volunteers purchased from the Regional Center of Blood Donation and Treatment in Kraków. The Regional Center of Blood Donation and Treatment deidentified blood materials as appropriate for the confidentiality assurance of human subjects. Thus, this study adheres to relevant exclusions from the approval of human subjects. The blood cells were separated in a density gradient of Ficoll-Paque Plus (GE Healthcare, Chicago, IL, USA). Freshly isolated hPBMC were cultured in RPMI-1640 with 20% (v/v) FBS and antibiotics (100 U/mL Penicillin, 100 μ g/mL Streptomycin) and hPMN in RPMI-1640 with 10% (v/v) FBS and antibiotics. Cells isolated from at least five donors were analyzed.

Human HEK Reporter Cell Lines Overexpressing Toll-Like Receptors (TLR)

Human TLR4/NF- κ B-SEAP reporter HEK293 cells, human TLR5/NF- κ B-SEAP reporter HEK293 cells, human TLR2+TLR1/NF- κ B-SEAP reporter HEK293 cells and human TLR2+TLR6/NF- κ B-SEAP reporter HEK293 cells were from InvivoGen (San Diego, CA, USA). Cells were cultivated in DMEM GlutaMAXTM containing 4.5 g/L with 10% (v/v) FBS and selective antibiotics provided by InvivoGen.

Cell Viability Assays

P388D1, RAW 264.7, HepG2 cells were seeded on a 96-well plate at the density of 5×10^3 or HEK293/TLRs at the density of 2.5×10^4 cells per well in 100 μ L of cell culture medium. Next, after overnight incubation (P388D1, RAW 264.7, and HepG2) or directly after seeding (HEK293/TLRs), 10 μ L of PEG solutions or PBS (as negative control; 100% of cell viability) were transferred to subsequent well. Cell viability was measured after 24 h (HEK293/TLRs) or 48 h (P388D1, RAW 264.7, and HepG2) of incubation using the microplate reader and MTT assay according to the standard protocol.²⁶

The mPN cells were seeded at the density of 6×10^4 /well on a 96-well plate in 100 μ L of growth medium. hPBMC and hPMN were seeded directly after isolation at the density of 1×10^5 cells per well in 100 μ L of cell culture medium. Subsequently, 10 μ L of PEG solutions (the final PEG concentration was 5 mg/mL) or PBS were transferred to wells.

After 24 h (mPN, hPMN) or 48 h (hPBMC) of incubation, cell viability was evaluated by ATPlite luminescence assay according to the manufacturer's procedure (PerkinElmer). Chemiluminescence intensity was measured using a microplate reader.

Measurement of Nitrate Oxide in Culture Media Collected from Monocyte-Macrophage Cells

P388D1 cells were transferred in 100 μ L of cell culture medium at the density of 1.5×10^4 per well on a 96-well plate. After overnight cultivation, the cell growth medium was replaced by 100 μ L of DMEM with 4.5 g/L glucose, 2% FBS, and antibiotics. Next day: 1) 10 μ L of PEG solutions (the final PEG concentration was 5 mg/mL), PBS or 100 ng/mL LPS (as positive control), or 2) 10 ng/mL IFN- γ (enhancer of macrophage immune stimulation) + 10 μ L of PEG solutions, PBS or 100 ng/mL LPS were pipetted to subsequent wells. After 24 h of incubation, nitrate levels were measured after mixing 100 μ L of collected media with 100 μ L of Griess reagent (1% (w/v) sulfanilic acid/0.1% (w/v) N-(1-naphthyl) ethylenediamine dihydrochloride] in 2.5% [v/v] H_3PO_4). The absorbance was measured at 545 nm using a microplate reader.

Assessment of Intracellular Reactive Oxygen Species

Analysis Using a Microplate Reader

Cells were seeded on the 96-well black plate with transparent bottoms at a density of 1×10^4 (P388D1); 1×10^4 (RAW 264.7); 1.5×10^4 (HepG2); 1×10^5 (hPMN) per well in 100 μ L of growth medium. The hPMN were transferred to the plate directly in the medium dedicated for measuring fluorescence intensity - 10% (v/v) FBS, DMEM without phenol red (noPRed), antibiotics, and fluorescence probes: 25 μ M dichloro-dihydro-fluorescein diacetate (DCF) or 10 μ M dihydrorhodamine (DHR). At the same time, 10 μ L of PEG solutions (the final PEG concentration was 5 mg/mL), PBS, or ROS stimulators at a final concentration of 100 nM PMA (phorbol 12-myristate 13-acetate) or 1 mM H_2O_2 were added to the wells.

P388D1, RAW 264.7, and HepG2 were left in the incubator overnight. Next day the growth media were replaced by fresh medium dedicated to the measurements of fluorescence intensity 10% (v/v) FBS, DMEM noPRed (for P388D1 and RAW 264.7 with 4.5 g/L and HepG2 cell with 1 g/L of glucose) and antibiotics supplemented with fluorescence probe 25 μ M DCF, or 10 μ M DHR. At the same time, 10 μ L of PEG solutions, PBS, or ROS stimulator at a final concentration of 1mM H_2O_2 were added to the wells. Immediately after adding ROS stimulants, plates were transferred to the microplate reader (the final volume in each well was the same). Then, kinetic fluorescent measurements were conducted for 4 h, and the fluorescence intensity was measured in 15-minute intervals. The excitation and emission wavelengths for the individual probes were as follows: DCF 470 nm/535 nm and DHR 485 nm/525 nm.

Flow Cytometry

Human peripheral blood mononuclear cells were transferred to the 96-well, V-shape plate at the density of 1×10^5 per well in 100 μ L dedicated to the measurements of fluorescence intensity 20% (v/v) FBS, DMEM noPRed and supplemented with fluorescence probe DCF (25 μ M), or (10 μ M) DHR. At the same time, 10 μ L of PEG solutions (the final PEG concentration was 5 mg/mL), PBS, or ROS stimulator PMA (100 nM) were added to the wells. Cells were transferred into the incubator and incubated for 3 h with ROS stimulants. Subsequently, hPBMC were centrifuged (400 \times g/5 minutes; 4°C) and stained with 200 μ L of 2.5 μ g/mL 7-AAD (7-amino actinomycin D) in PBS to exclude death cells. Cells were analyzed using a BD FACSCalibur flow cytometer supported by CellQuestPro software (Becton Dickinson, USA). The results were processed with FlowJo software (Becton Dickinson, USA). The mean fluorescence intensity (MFI) of DCF and DHR was measured on the FL-1H channel. Dead cells were excluded from the analysis based on forward scatter (FSC) and FL3-H plots. The gating strategy is shown in [Figure S1](#).

Detection of Cytokines

Subsequent cells were seeded at the density of 1.5×10^4 (P388D1), 6×10^4 (mPN), and 1×10^5 (hPMN and hPBMC) in 100 μ L of growth medium. Directly after transferring mPN, hPMN, and hPBMC to a 96-well plate, stimulating agents were added: 1)

10 μ L of PEG solutions (the final PEG concentration was 5 mg/mL); 2) 10 μ L of PBS or 3) LPS at a final concentration of 100 ng/mL. P388D1 cells were left in the incubator overnight after seeding. Then, the medium was replaced with 100 μ L of fresh one containing 2% (v/v) FBS, DMEM, and antibiotics. On the following day, stimulating agents were added: 1) 10 μ L of PEG solutions, 2) 10 μ L of PBS, or 3) LPS at a final concentration of 100 ng/mL. After 24 h (P388D1, mPN, and hPMN) or 48 h (hPBMC) incubation, the media above cells were collected and stored at -20°C . Before the cytokine examination, the tested media were refrozen. The cytokine concentrations (mouse: IL-1 α , IL-1 β , IL-6, IL-10, IL-12p70, IL-17A, IL-23, IL-27, MCP-1, IFN- β , IFN- γ , TNF- α , and GM-CSF; human: IL-1 β , IFN- α 2, IFN- γ , TNF- α , MCP-1, IL-6, IL-8, IL-10, IL-12p70, IL-17A, IL-18, IL-23, IL-33) were analyzed using LEGENDplex Mouse Inflammation Panel (13-plex) or Human Inflammation Panel 1 (13-plex) kit (Biolegend) and the BD LSRFortessa flow cytometer. The results were analyzed using LEGENDplex software (Biolegend).

Immunofluorescence Staining of Released Neutrophil Extracellular Traps (NET)

hPMN (1×10^6 cells per sample in 1 mL of growth medium) were seeded on 0.01% poly-L-lysine-coated (Sigma, St. Louis, MO, USA) glass coverslips placed in a 12-well culture plate. After 1 h, dedicated to cell adhesion, the cells were stimulated with 1) 100 μ L of PEG solutions (the final PEG concentration was 5 mg/mL), 2) 100 μ L of PBS, or 3) PMA at a final concentration of 100 nM. Next, after 3 h of incubation, cells were fixed in a 4% (v/v) solution of methanol-free formaldehyde (Thermo Fisher Scientific, Waltham, MA, USA) in PBS for 15 min at RT. Subsequently, glass coverslips were washed 3 times with PBS, blocked and permeabilized in the blocking buffer (5% (v/v) FBS, 0.3% (v/v) Triton X-100 in PBS) for 1 h at RT and incubated with recombinant anti-myeloperoxidase antibody (Abcam, Cambridge, UK) diluted at a concentration of 2.34 μ g/mL in the blocking buffer overnight at 4°C . The next day, the cells were washed 3 times with PBS and incubated with Alexa Fluor-647 goat anti-rabbit antibodies (Invitrogen, Waltham, MA, USA) diluted in blocking buffer for 1.5 h at RT. Finally, after washing with PBS, cells' nuclei were stained with 4,6-diamidino-2-phenylindole (DAPI) (Thermo Fisher Scientific, Waltham, MA, USA), and the samples were mounted onto slides in ProLong Glass Antifade Mountant (Thermo Fisher Scientific, Waltham, MA, USA). After 24 h, the samples were examined under an inverted fluorescent microscope Olympus IX83 supported with cellSens software (Evident Scientific, Japan). Image analysis was performed using ImageJ 1.53c (National Institutes of Health, Bethesda, MD, USA).

Analysis of PEG Interactions with Toll-Like Receptors (TLR)

The activation of selected TLR receptors was analyzed by measuring SEAP (secreted embryonic alkaline phosphatase) activity secreted to the culture media of reporter HEK293 cells. Human TLR4/NF- κ B-SEAP, TLR5/NF- κ B-SEAP, TLR2+TLR1/NF- κ B-SEAP and TLR2+TLR6/NF- κ B-SEAP reporter HEK293 cells were transferred on 96-well plate at the density of 2.5×10^4 in 100 μ L of HEK-Blue Detection Medium (prepared following the manufacturer's instructions). Next, 10 μ L of PEG solutions (the final PEG concentration was 5 mg/mL) or PBS was added to the medium. Positive controls were also prepared by adding 10 μ L of specific ligands at a final concentration of 10 ng/mL LPS for TLR4, 2 μ M CU-T12-9 (a small-molecule agonist for Toll-like receptor 2) for TLR2/TLR1 heterodimer, 1 ng/mL FSL-1 (synthetic diacylated lipoprotein) for TLR2/TLR6 heterodimer and 1 ng/mL flagellin for TLR5. Cells were incubated for 24 h; next, to measure the activity of SEAP, 90 μ L of cultured HEK-Blue Detection Medium were transferred to the fresh 96-well plate, and the absorbance was measured at 620 nm using a microplate reader.

Calcium Imaging

hPMN at a density of 0.5×10^6 cells per 0.5 mL of RPMI were pre-incubated in 37°C for 10 minutes with 1) 50 μ L of PEG 2 or mPEG 10 (the final PEG concentration was 5 mg/mL), or 2) 50 μ L of PBS. Then, the Ca^{2+} indicator Fluo-4 AM (Thermo Fisher Scientific, Waltham, MA, USA) was added to the cell suspension (kept in RPMI medium with or without PEG2/mPEG10) to achieve a final concentration of 2 μ M. The cells were immediately transferred to a flow chamber onto a coverslip coated with 0.01% poly-L-lysine and 20 μ g/mL laminin. After 20 minutes of incubation in RT, the flow chamber was mounted on a Leica DMI8 fluorescence microscope equipped with an HC PL APO 40x/1.30 OIL objective and a DFC7000GT camera (Leica, Germany). The Fluo-4-loaded cells were then washed with NaHEPES buffer

(containing 140 mM NaCl; 4.7 mM KCl; 10 mM HEPES; 1 mM $MgCl_2$; 10 mM glucose; 1.0 mM $CaCl_2$) in the presence of PEG2 or mPEG10 (at a final concentration of 5 mg/mL) or control conditions (without PEG). The Ca^{2+} -sensitive indicator was excited using an LED light source with maximum intensity at 490 nm, and green emission was collected (with an emission peak at 528 nm). A series of images were recorded with binning set at 5×5 (resolution: 384×288 pixels), and the time interval between two consecutive images was 2 seconds. The experiments were conducted without perfusion for the first 500 seconds when they were exposed to NaHEPES containing either PEG2 or mPEG10 or to NaHEPES alone (as a control). Then, as an internal quality control for cell functionality, 10 μM ATP was added by perfusion to the chamber for the last 100 seconds of the experiment. Only experiments with 10 μM ATP-induced consistent responses across all cells (via purinergic receptor signaling) were selected for downstream analysis.

Due to cell migration observed during the experiment, particularly with mPEG10, the TrackMate plugin in Fiji was employed as an automatic cell-tracking system to collect fluorescence signals from the migrating cells.^{27,28} In the experiment, single cells were tracked using the Laplacian of Gaussian detector in TrackMate. The parameters set included an estimated object diameter of 10 μm , preprocessing with a median filter, and sub-pixel localization. The Linear Assignment Problem (LAP) tracker was configured with a maximum linking distance of 10 μm between frames and a gap-closing distance of 10–15 μm . Segment merging was employed for rapidly migrating cells at high densities with a maximum distance of 10 μm . Only fluorescence data for cells consistently present in the field of view throughout the experiment were selected for further analysis. Fluorescence signals were quantified as F/F_{MIN} , where F_{MIN} represents the minimum signal observed for each cell during the experiment. The area under the curve was calculated from 0 to 500 seconds for each trace. To characterize the frequency and nature of calcium responses, we calculated the number of data points where F/F_{MIN} exceeded thresholds of 2 and 5 for each trace.

Statistical Analysis

In cytokine detection experiments, statistical significance was analyzed by two-way repeated measures (RM) ANOVA with Geisser-Greenhouse correction followed by Tukey's multiple comparison test. If there were missing values in groups (cytokine levels were below or above detection limits), a mixed-effects model (REML) was used instead of RM ANOVA. In the case of calcium imaging tests, statistical significance was assessed using the Kruskal–Wallis test, followed by Dunn's post hoc test. All analyses were performed in GraphPad Prism 10.

Results and Discussion

Tested PEG and mPEG are Not Toxic to Immune Cells and Hepatocyte Model Cells

Immune cells are particularly susceptible to direct contact with PEGylated therapeutics, regardless of their route of administration into the body. Interestingly, some data indicate that PEG can detach from the PEGylated nanomedicines immediately after administration, interact as a free PEG with various cells, and accumulate in phagocytes.²⁹ Schoenbrunn et al have shown that macrophages can actively capture 20 kDa mPEG, which eventually accumulates in aggregates within their cytoplasm. Furthermore, they confirmed that exposure of macrophages to mPEG 20 kDa in concentrations above 1 mg/mL leads to significant cell vacuolization compared to control cells.³⁰ Similarly, observations published by Fang et al indicated that subcutaneous or intravenous injections of free PEG resulted in an increased vacuolization in macrophages residing in the spleen, lymph nodes, lungs, and other tissues. Still, this phenomenon seemed reversible and was likely involved in the clearance of PEG from the body.³¹ Since most research evaluating the cytotoxicity of PEG and PEGylated nanopharmaceuticals focused on only one type of PEG, we investigated the effects of PEG and mPEG of different molecular weights on mouse and human cells. Our research was initiated by exploring the direct interactions of polyethylene glycols with immune cells, particularly phagocytes. As presented in Figures 1 and S2, exposing a range of mouse (P388D1, mPN, RAW 264.7) and human (hPBMC, hPMN) immune cells to the tested PEG and mPEG solutions did not affect cell viability.

Hepatocytes represent another cell type highly vulnerable to PEG, owing to the discontinuous nature of liver blood vessel walls and the pivotal role of the liver in the metabolism and removal of various compounds. This anatomical feature permits the substances in the blood to come into contact with hepatocytes and potentially leads to the accumulation of PEGylated

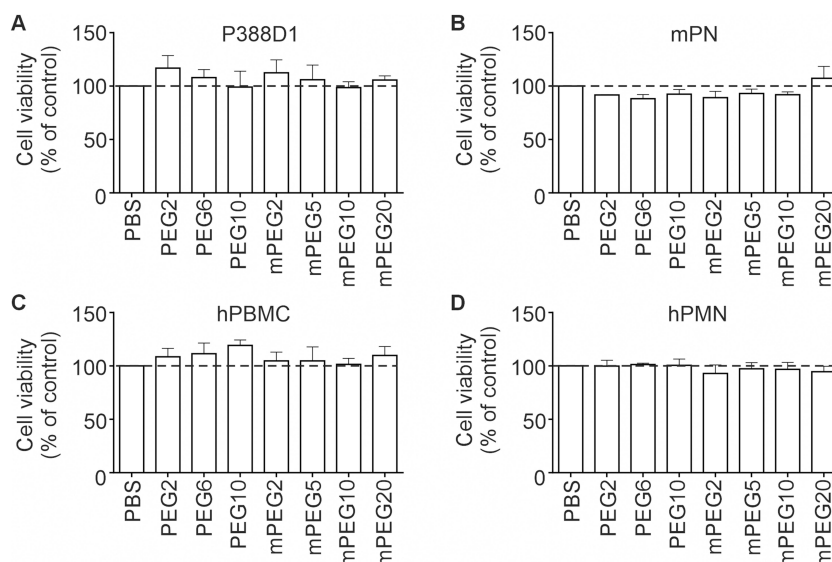


Figure 1 Polyethylene glycols do not affect the viability of mouse and human immune cells.

Notes: The cells were incubated for 24 (mPN, hPMN) or 48 (P388D1, hPBMC) hours in media supplemented with PBS, PEG, or mPEG solutions. The viability of P388D1 cells was analyzed using MTT (A). For mPN (B), hPBMC (C), and hPMN (D), the ATPlite test was performed. The data are presented as an average of 3 independent experiments \pm SD.

Abbreviations: P388D1, mouse monocyte/macrophage cell line; mPN, mouse neutrophils differentiated from mouse neutrophil progenitors; hPBMC, human peripheral blood mononuclear cells; hPMN, human polymorphonuclear neutrophils; PEG, polyethylene glycol; mPEG, methoxy polyethylene glycol.

therapeutics within these cells.^{32,33} Furthermore, our previous studies with PEGylated polyelectrolyte nanocapsules indicated that these nanocarriers are eliminated from the body via hepatobiliary clearance.²³ Therefore, here we have also evaluated the influence of PEG and mPEG on HepG2 cells, a model of human hepatocytes. Our results showed that PEG and mPEG do not exhibit cytotoxicity towards HepG2 cells (Figure S2). Collectively, we have established that neither PEG nor mPEG compromises the viability of either immune cells or hepatocytes.

ROS Production is Not Increased in Response to PEG and mPEG

Generated predominantly in mitochondria but also in other cellular compartments, such as peroxisomes and the endoplasmic reticulum, reactive oxygen species (ROS) are implicated in inducing oxidative stress when their levels surpass the cellular antioxidative capacity but also play multifaceted roles in cellular physiology and signaling. Importantly, increased production of ROS in response to various proinflammatory factors allows phagocytic cells to eliminate pathogens.³⁴ External factors, including nanomaterials and their chemical constituents, can markedly elevate intracellular ROS generation, resulting in oxidative imbalance, damage to cellular macromolecules, cell dysfunction, and even death. The overproduction of ROS is regarded as a primary contributor to nanotoxicity.³⁵ To assess ROS production in the cells exposed to PEG and mPEG, we utilized two ROS-sensitive fluorescent probes: dichloro-dihydro-fluorescein diacetate (DCF) and dihydrorhodamine (DHR). At the same time, we employed two different experimental approaches to investigate the redox state of cells exposed to the tested PEG and mPEG. ROS production in hPMN, HepG2, and mouse P388D1 and RAW 264.7 cells was measured over 4 hours at 15-minute intervals, resulting in graphs illustrating ROS formation's kinetics. Additionally, ROS levels in hPBMC cells were determined after 3 hours of incubation with PEG and mPEG using flow cytometry. As depicted in Figures 2 and S3–S5, the kinetics of ROS generation in cells exposed to polyethylene glycols were similar to those observed in cells incubated in a medium with PBS. An increase in ROS levels was present only in cells incubated with ROS-inductors PMA or H₂O₂. ROS levels in hPBMC cells, determined by cytometric measurements after 3 hours of incubation with PEG or mPEG, were also consistent with the results obtained via kinetic fluorescence intensity measurements (Figure 3). The level of ROS in cells, represented by mean fluorescence intensity (MFI), was similar in PEG- and mPEG-treated cells as in control cells. Upon exposure to PMA, which was used as an oxidative stress inducer, a more than twofold increase in intracellular ROS levels was observed for each probe, confirming the appropriate responsiveness of the probe to ROS.

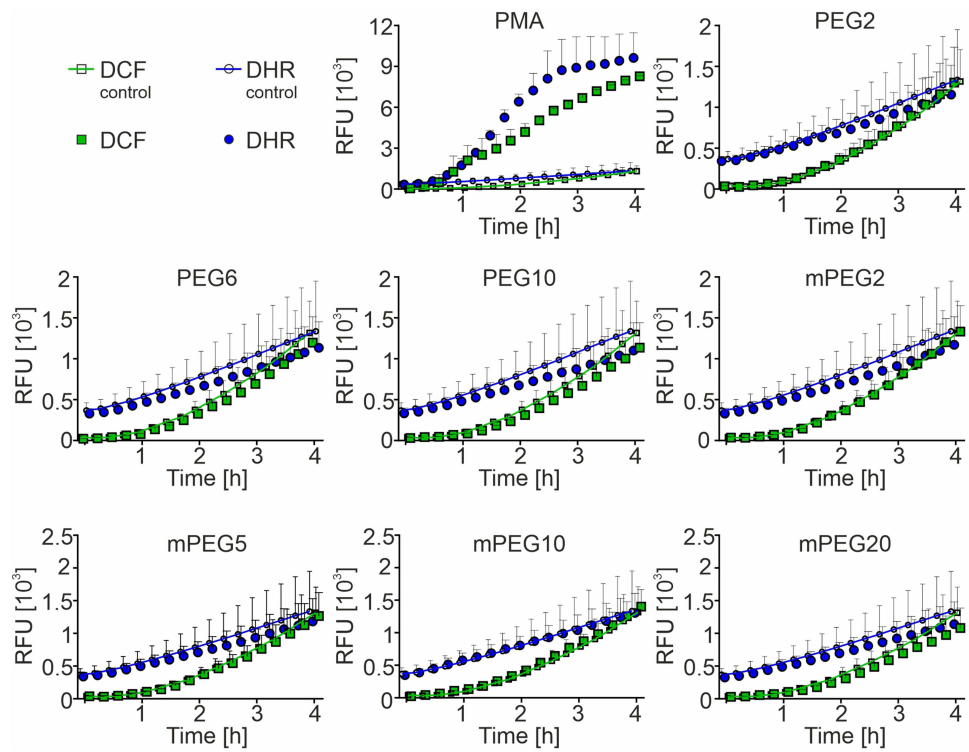


Figure 2 The intracellular ROS level in human neutrophils is unaffected by polyethylene glycols.
Notes: Human neutrophils were mixed with media containing ROS-sensitive fluorescent probes DCF and DHR. Next, the medium was enriched with PBS (negative control), PMA (positive control of ROS production), or PEG and mPEG solutions. Immediately after the addition of stimulants, the fluorescence intensity of DCF (470 nm/535 nm) and DHR (485 nm/525 nm) was measured. The measurement was carried out for 4 hours at 15-minute intervals, maintaining a constant temperature of 37°C. Data were presented as an average of two independent experiments \pm SD.
Abbreviations: DCF, dichloro-dihydro-fluorescein diacetate; DHR, dihydrorhodamine; PEG, polyethylene glycol; mPEG, methoxy polyethylene glycol; PMA, phorbol 12-myristate 13-acetate.

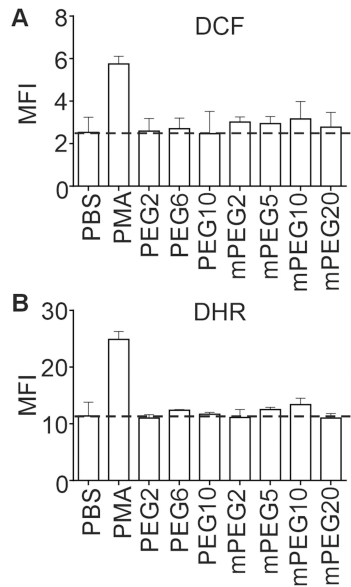


Figure 3 Analysis of polyethylene glycols influence on intracellular ROS levels in hPBMC.
Notes: Cells were incubated for 3 hours with PBS, PMA, PEG, or mPEG solutions and specific fluorescent probes (A) DCF or (B) DHR. Reactive oxygen species were determined by fluorescence measurement using a flow cytometer. Only living cells were selected for analysis (see the gating strategy in Figure S1). The data are presented as mean MFI from three independent experiments \pm SD.
Abbreviations: DCF, dichloro-dihydro-fluorescein diacetate; DHR, dihydrorhodamine; PEG, polyethylene glycol; mPEG, methoxy polyethylene glycol; PMA, phorbol 12-myristate 13-acetate; MFI, mean fluorescence intensity.

The existing data on PEG as an inducer of ROS formation are ambiguous. The polyoxyethylene chain of PEG is prone to metal- or light-induced decomposition, starting the exogenous ROS production. Given that PEG can be taken up by the cells where it has pro-oxidative properties, intracellular ROS production may also occur.^{36–38} The stimulating effect of free PEG on ROS production has been previously observed in erythrocytes while testing the application of this polymer for cryopreservation and was linked primarily to PEG-induced changes in the functional activity of essential membrane proteins involved in erythrocyte ion transport.³⁹ Earlier studies presented by Hak-Joon-Sang demonstrated that depending on the substrate covalently bound with the PEG, its effect on ROS production differs.³⁸ Yet other data suggest that free PEG decreases ROS in damaged cells and injured tissues and induces cell membrane repair.⁴⁰ However, our results in this work do not indicate the oxidative activity of tested PEG or mPEG.

Specific PEG and mPEG Have Proinflammatory Activity Independent of TLR Signaling

Immune cell-derived nitrate oxide (NO) and proinflammatory cytokines are critical factors in the inflammatory response. The excessive secretion of NO and proinflammatory cytokines can increase the risk of tissue injuries and the development of various diseases, including rheumatoid arthritis and atherosclerosis.⁴¹ The proinflammatory activity of tested polyethylene glycols was first verified on mouse monocyte-macrophage cells. P388D1 and RAW 264.7 cells were exposed for 24 hours to polyethylene glycols alone or polyethylene glycols in the presence of IFN- γ , a known enhancer of the inflammatory response of cells to various factors, allowing sensitive detection of NO production by inducible NO synthase (iNOS). **Figure 4** shows that upregulated NO production was observed only for P388D1 cells stimulated with LPS or LPS+IFN- γ or for RAW 264.7 cells stimulated with LPS+IFN- γ (activators of inflammatory response). Moreover, analysis of cytokine production by P388D1 and mouse neutrophils differentiated from mouse neutrophil progenitors (mPN) demonstrated that PEG or mPEG solutions did not induce the expression of proinflammatory cytokines (**Figures S6 and S7**). The responsiveness of the cells to proinflammatory stimuli was validated by exposure to LPS (P388D1) or PMA (mPN), which led to an increased expression of specific cytokines: TNF- α , IL-6 (**Figure S8**). Liu et al previously observed elevated NO and cytokine production by RAW264.7 cells treated with PEGylated gold nanoparticles. However, the absence of a comparison with non-PEGylated gold nanoparticles in these studies makes it challenging to definitively attribute this effect to PEG alone.⁴²

Cytokine production by human PMN and PBMC was also analyzed. Interestingly, we observed different cytokine responses to PEG depending on blood donors. Neutrophils isolated from some volunteers and treated with mPEG2, or especially with mPEG10, upregulated secretion of IL-8 (**Figure 5**), a chemokine important in activating and attracting leukocytes, predominantly neutrophils, to the inflammation foci. Similarly, neutrophils isolated from some donors secreted higher levels of IL-18 after treatment with PEG10, mPEG2, or mPEG10. Furthermore, for all PEG or mPEG, upregulated production of IL-33 by hPMN from some volunteers was also demonstrated. At the same time, we observed that hPBMC isolated from some donors responded to specific PEG, but mainly to specific mPEG, increasing the

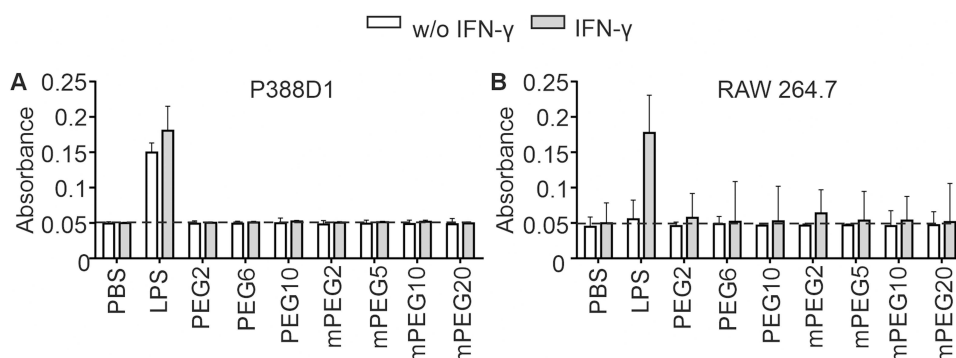


Figure 4 Polyethylene glycols do not stimulate inducible nitric oxide synthase expression in mouse monocytes-macrophages.

Notes: The Griess test measured nitric oxide levels in cultured media after 24 hours of (A) P388D1 and (B) RAW 264.7 cells incubation in a medium supplemented with PBS (negative control), LPS, LPS combined with IFN- γ (positive controls of NO production), PEG or mPEG solutions alone or combined with IFN- γ . The data are presented as an average of three independent experiments \pm SD.

Abbreviations: P388D1 and RAW 264.7, mouse monocyte/macrophage cell line; PEG, polyethylene glycol; mPEG, methoxy polyethylene glycol; LPS, lipopolysaccharide; w/o, without.

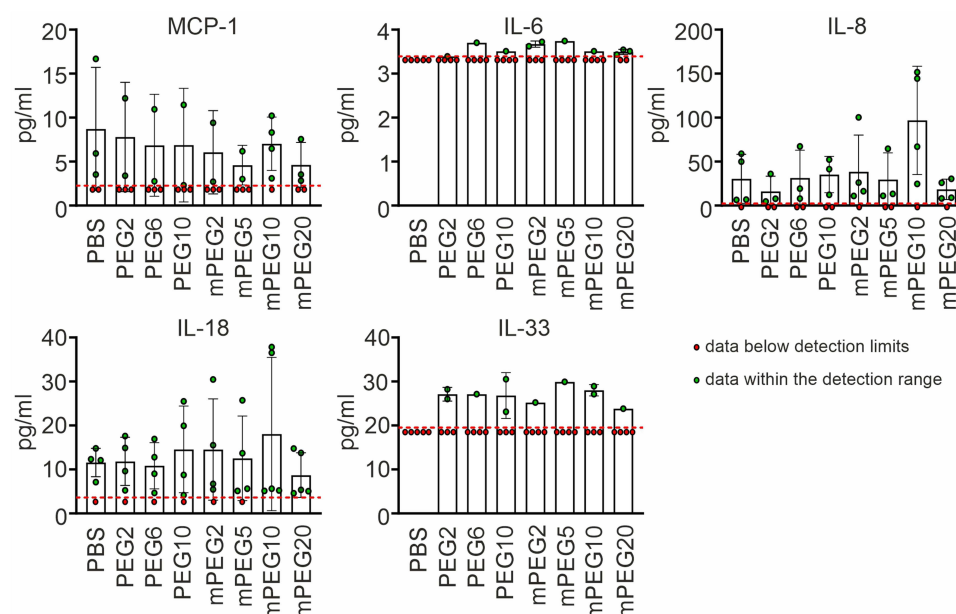


Figure 5 Human neutrophils stimulated by polyethylene glycols upregulate cytokines.

Notes: Human neutrophils were incubated for 24 hours in media containing PBS (negative control), PEG, or mPEG solutions. Media were then collected, and cytokine concentrations were determined using the human LEGEND/Plex Inflammation Panel and flow cytometry. The graphs show the means of the data within detection range \pm SD. The experiment was repeated 5 times with cells isolated from different donors. Red dots represent data below the detection range.

Abbreviations: PEG, polyethylene glycol; mPEG, methoxy polyethylene glycol.

expression of IFN- α 2, IFN- γ , TNF- α , MCP-1, IL-8, IL-17A, IL-23, IL-33, IL-12p70, IL-6, IL-18, IL-10 (Figure 6). The most potent proinflammatory activity against hPBMC demonstrated mPEG20 (Figure 6).

The concentration of some cytokines was under the detection limits for all tested samples. For hPMN, under the detection limit were IL-1 β , IFN- α 2, IFN- γ , TNF- α , IL-10, IL-12p70, and IL-23 and for hPBMC, the concentration of IL-1 β . Detection limits of various cytokine concentrations are presented in Figure S9. Our results suggest a correlation between cells isolated from different volunteers and sensitivity to PEG or mPEG. Reports have previously revealed the genetic susceptibility to develop a humoral response to PEG manifesting in IgM production.⁴³ Here, we postulate that other immune reactions to PEG, such as cytokine production, may also depend on the differential sensitivity of human immune cells from different donors to PEG. Perhaps, as in the case of the antibody response to PEG, individual susceptibility to recognize and respond to PEG predicts the activation of the innate immune response to PEG. However, this hypothesis requires profound experimental verification.

It is poorly understood how cytokines are produced in vitro and in vivo in response to free PEG or PEGylated nanomaterials. Our previous in vivo studies showed that PEGylated polyelectrolyte nanocapsules induced increased secretion of proinflammatory cytokines such as IL-12p70, IFN γ , IFN β , IL-17 α , GM-CSF, and IL-6.²³ Notably, Schoenbrunn et al's studies on the proinflammatory activity of 20 kDa PEG did not result in marked increases in cytokine secretion by human monocyte-derived macrophages.³⁰

To elucidate the mechanism of PEG's proinflammatory effects, Amer et al demonstrated that synthetic PEG hydrogels could stimulate myeloid differentiation primary response gene (MyD88) signaling in vitro and in vivo.⁴⁴ MyD88 is a critical adaptor protein mediating most Toll-like receptor (TLR) signaling, resulting in the induction of inflammatory response. Moreover, since secretion of various cytokines, including IL-12p70, IL-23, and IL-8 expression, often occurs after TLR activation, we verified if tested PEG acts as TLR ligands. In the presented studies, we used reporter HEK-blue cells overexpressing TLR4, TLR5, TLR2+TLR1, and TLR2+TLR6, but we did not observe activation of any of these receptors by PEG or mPEG (Figure 7).^{45,46}

The hypothesis that PEG or PEGylated nanomaterials signal via receptors expressed on the surface of various cells, including phagocytes, has already been proposed, with TLRs, scavenger receptors, and lipoprotein receptors identified as the most critical candidates.^{47,48} Studies performed on mouse macrophages have suggested that scavenger and

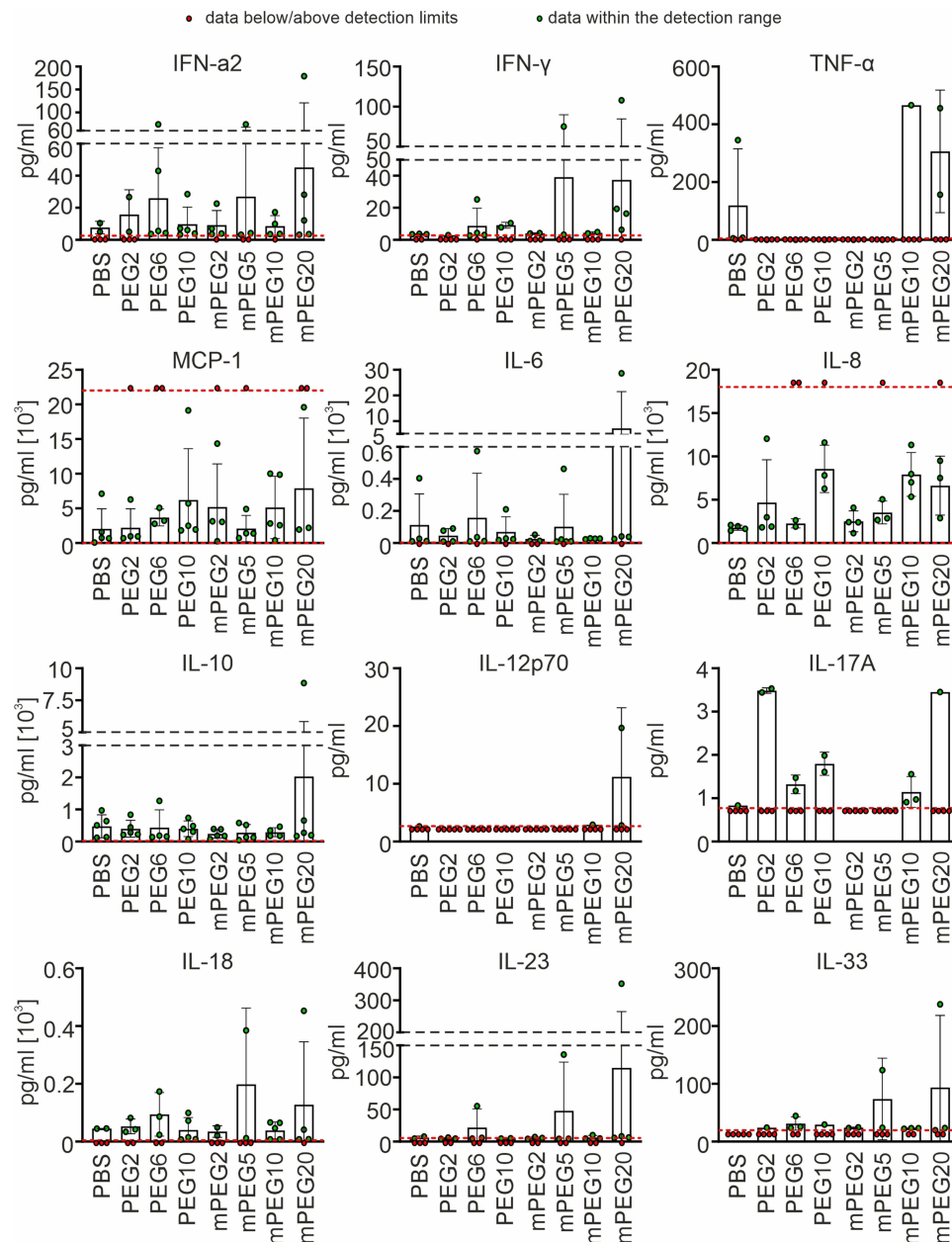


Figure 6 Human peripheral blood mononuclear cells were stimulated with polyethylene glycol solutions to produce cytokines.

Notes: Human PBMC were incubated for 48 hours in media containing PBS (negative control), PEG, or mPEG solutions. Cytokine concentrations released to the cultured media were determined using the human LEGEND/Plex Inflammation Panel and flow cytometry. The graphs show the means of the data within detection range \pm SD. The experiment was repeated 5 times with cells isolated from different donors.

Abbreviations: PEG, polyethylene glycol; mPEG, methoxy polyethylene glycol.

lipoprotein receptors are targets for PEGylated nanomaterials. Moreover, subsequent signaling through these receptors did not result in the upregulated secretion of proinflammatory cytokines. These observations suggest that, at least in mouse macrophages, PEGylated nanomaterials are recognized more as lipoproteins than pathogens.⁴⁸

Surprisingly, our studies revealed a prominent difference in vitro responses between mouse and human cells to specific PEG or mPEG. Mouse cells exposed to PEG or mPEG do not develop an inflammatory response, contrary to human immune cells that are more sensitive to PEG and mPEG. Our results also suggest that the responses of human cells are not dependent on TLR signaling.

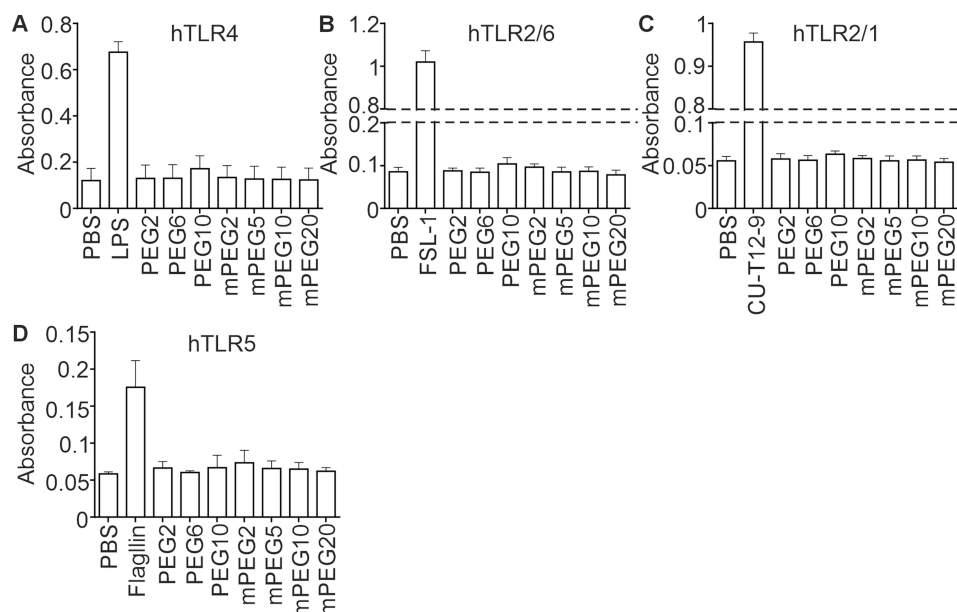


Figure 7 Polyethylene glycols are not ligands for human Toll-like receptors.

Notes: Analysis was performed using HEK-blue reporter cells stably expressing (A) hTLR4, (B) hTLR2/TLR1, (C) hTLR2/TLR6, or (D) hTLR5. The cells were exposed to PBS, PEG, mPEG solutions, or specific TLR ligands (LPS, FSL-1, CU-T12-9, or flagellin). NF- κ B activation resulting from TLR activation was analyzed after detecting Secretory Embryonic Alkaline Phosphatase activity (SEAP).

Abbreviations: PEG, polyethylene glycol; mPEG, methoxy polyethylene glycol; TLR, Toll-like receptors; LPS, lipopolysaccharide; FSL-1, synthetic diacylated lipoprotein; CU-T12-9, small-molecule agonist for Toll-like receptor 2.

Neutrophils Release Extracellular Traps (NET) in Response to mPEG10

NET formation is a hallmark of neutrophil activation by various stimuli.⁴⁹ This process aids in eliminating pathogens during infection; however, excessive NET release can damage tissue or trigger autoimmune reactions.^{50–52} Some nanomaterials, including PEGylated ones, have demonstrated potential as inducers of NET release. In most cases described, this was directly preceded by increased ROS production.⁵³ So far, no information exists on the stimulation of NET formation by free PEG. Of all the types of PEG we tested, only mPEG10-induced NET release in human neutrophils. However, since we observed no increase in ROS production in cells exposed to mPEG10, we concluded that it triggers ROS-independent NETosis (Figure 8). Interestingly, as shown in Figure 5, only mPEG10 induced increased IL-8 secretion by neutrophils. IL-8, a chemokine, primarily attracts neutrophils to infection, inflammation, and damaged tissue sites and subsequently promotes NET formation.^{54,55}

mPEG10 Triggers Ca^{2+} Signals in Human Neutrophils

Ca^{2+} signaling controls the vast majority of cellular processes, and accumulating evidence suggests that it may also play an essential role in regulating neutrophil functions.⁵⁶ Ca^{2+} signals orchestrate the response to various stimuli, including pathogen or damage-associated molecular patterns (PAMPs, DAMPs) and cytokines or chemokines released by immune cells.^{56–59} Several studies suggest an increase in intracellular Ca^{2+} is crucial for NETosis induced by PMA, with chelation of intracellular Ca^{2+} using BAPTA-AM significantly inhibiting NET formation.^{60,61} However, the effect of chelating extracellular Ca^{2+} with EGTA has shown less consistency across different studies. While it is clear that the intracellular Ca^{2+} pool is essential for NETosis, the role of extracellular Ca^{2+} and its influx remains less obvious. To explore if mPEG10 triggers Ca^{2+} signals in neutrophils – which could be a potential mechanism contributing to its proinflammatory effects, including enhanced cytokines secretion and NET formation – we examined Ca^{2+} signaling dynamics in hPMN exposed to mPEG10. In this experiment, control cells were treated with PBS and washed with NaHEPES (Figure 9A) and as a control PEG, we selected PEG2, which did not exhibit proinflammatory activity in our experiments (Figure 9B). A 20-minute incubation of hPMN with mPEG10 (Figure 9C) resulted in more pronounced Ca^{2+} responses, primarily

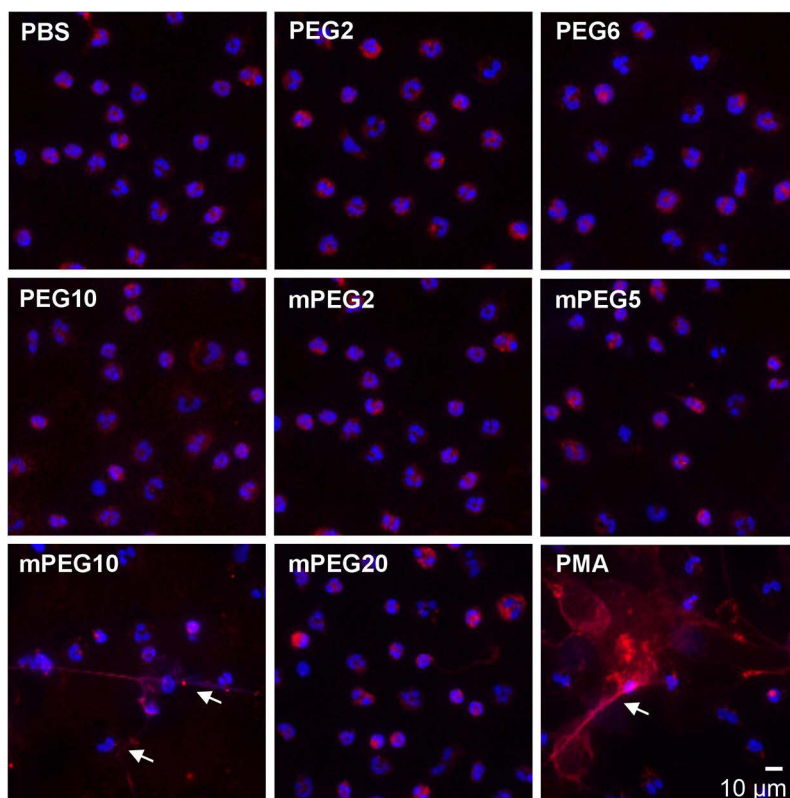


Figure 8 Neutrophil extracellular traps were released in response to mPEG10.

Notes: Human PMN was incubated in a control medium (negative control, with PBS) with PEG, mPEG solutions, or PMA (stimulator of NET formation) for 3 hours. The cellular DNA was stained with DAPI (blue), and myeloperoxidase was stained with specific antibodies (red). White arrows indicate NET. The cells were imaged using fluorescence microscopy.

Abbreviations: PEG, polyethylene glycol; mPEG, methoxy polyethylene glycol; PMA, phorbol 12-myristate 13-acetate.

transients with occasional baseline elevations, compared to controls: PEG2 or cells incubated with PBS and washed with NaHEPES only.

hPMN incubated with mPEG10 showed significantly larger response areas compared to both controls (Figure 9D). The magnitude of the Ca^{2+} responses was also significantly greater in cells incubated with mPEG10 than in those treated with PEG2 or in the PBS/NaHEPES control, as demonstrated by the average number of data points exceeding thresholds of $F/F_{\text{MIN}} > 2$ and > 5 (Figure 9E and F).^{39,62} However, our study is the first to show potentiated Ca^{2+} signaling in PEG-treated neutrophils.

Study Limitations

Our analysis was based on human blood cells isolated from a limited number of donors. Due to the volunteer's genetic susceptibility to PEG, our observations vary depending on the donor.⁴³ For instance, we observed cytokine levels, cell viability, and cell morphology variations among individual volunteers. For this reason, it was sometimes impossible to demonstrate statistically significant differences between some groups. However, we observed differences among individual volunteers. Therefore, larger groups of donors and simultaneous analysis of the genetic background should be considered for further studies. Additionally, we observed data points below or above the detection range in cytokine detection experiments for some samples. This resulted in a different number of replicates within groups that could be included in the statistical analysis.

Our research has underscored the potential impact of technical issues during leukocyte isolation or early development of inflammation in the donor's body since they could lead to endogenously high stimulation of hPBMC or hPMN, as evidenced by elevated cytokine levels in the medium of control cells.

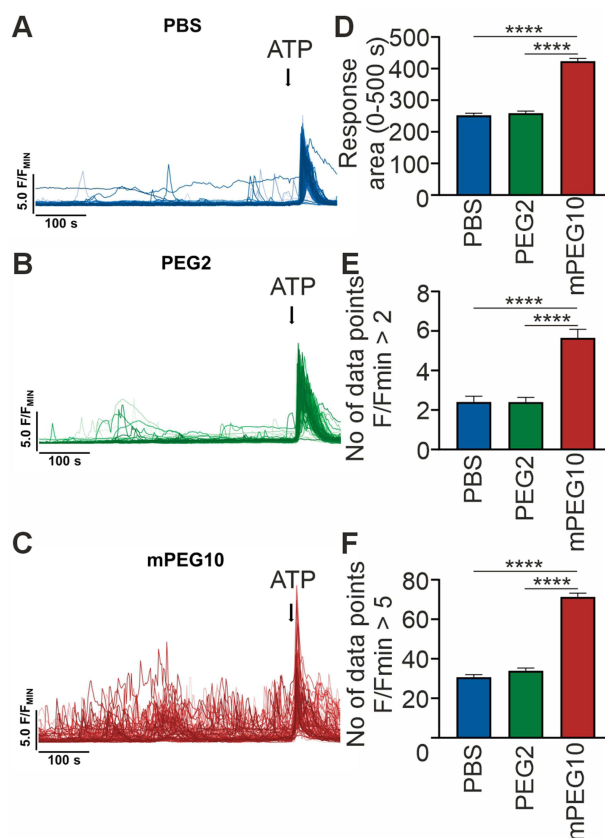


Figure 9 mPEG10 induces Ca^{2+} signals in hPMN.

Notes: (A–C) Representative traces of Ca^{2+} responses from hPMN treated with (A) PBS ($n = 109$), (B) PEG2 ($n = 167$), and (C) mPEG10 ($n = 89$). The addition of $10 \mu\text{M}$ ATP, used as a positive control, is indicated by a black arrow. (D) Chart comparing the average areas under the Ca^{2+} response curves for each treatment. (E and F) Charts depicting the average number of data points exceeding the set thresholds of $\text{F}/\text{F}_{\text{min}} > 2$ (E) and > 5 (F). Data shown in D–F are from five independent isolations of hPMN ($N = 5$), with totals of 1217 cells for PBS, 1385 for PEG2, and 1264 for mPEG10. Results are shown as means \pm SEM. **** $p < 0.0001$.

Abbreviations: AUC, area under the curve; PEG, polyethylene glycol; mPEG, methoxy polyethylene glycol; No, number.

The complexity of our research field is further highlighted by the variety of methods available for blood cell separation, such as different density gradient media and with or without red cell lysis. The choice of separation method can significantly impact the response of isolated cells to various stimuli, making it challenging to compare ex vivo data obtained by different groups. This complexity underscores our research community's need for standardized protocols and collaborative efforts.⁶³

Moreover, we are aware that the toxicity of PEG strongly depends on the type of compound (ie, nanoparticles or protein) to which the PEG has been attached. Therefore, toxicity testing is always required for newly designed PEGylated therapeutics. This may suggest that toxicity analysis of free PEG is not necessary. However, our results are essential in the context of the hypothesis of potential detachment of PEG from the PEGylated therapeutic after dosing and accumulation of free PEG chain in the body. In addition, there has recently been a proposal to administer 40 kDa-free PEG intravenously to patients as pre-treatment to inhibit the induction of anti-PEG antibodies. This proposal is based on the assumption that free PEG may act as a decoy, diverting the immune system's attention from the PEGylated therapeutic. Our findings support this hypothesis and suggest that further studies are needed to evaluate the safety and efficacy of this approach.⁶⁴ This underlines the importance of free PEG toxicity evaluation.

Conclusion and Future Prospects

Our research has significant implications as it explores the in vitro proinflammatory activity of specific PEG and mPEG, which are widely used in nanomedicine. Among all the polyethylene glycols tested, we observed notable proinflammatory properties for mPEG10 and mPEG20. We demonstrated that mPEG10 induces cytokine production by human

immune cells and the formation of neutrophil extracellular traps, possibly driven by Ca^{2+} signaling. However, the precise mechanism of this effect requires further investigation. Various types of mPEG are currently employed in nanomedicine, such as mPEG10, which is used to produce recombinant uricase (Krystexxa, Horizon). Patients taking this medication have reported side effects akin to those associated with other PEGylated nanomaterials, including allergic reactions, fever, cough, and sore throat.³

The use of PEGylated nanopharmaceuticals has undoubtedly contributed to advances in medicine. However, substances intended to be inert within the body can provoke side effects or worsen the patient's condition under certain conditions or doses. Therefore, understanding the immunotoxicity of PEGylated therapeutics or the immunotoxicity of specific components used for their synthesis is essential in the context of their safe use in medicine. Unfortunately, the evaluation of the toxicity of PEGylated nanomaterials, including their immunotoxic effects, primarily emerges during clinical trials. It highlights the critical need for more comprehensive preclinical research. Therefore, developing sensitive and reliable in vitro, in vivo, and future in silico models is crucial to swiftly identify potentially immunotoxic candidates among PEGylated nanopharmaceuticals before they reach clinical testing.

Funding

This work was supported by the Grant for Young Researchers no. MNS 11/2020 to AH funded by the Faculty of Biochemistry, Biophysics and Biotechnology of the Jagiellonian University in Kraków. The work of JJL and PEF was supported by the National Science Centre of Poland (Narodowe Centrum Nauki, NCN) under the OPUS project No. 2019/33/B/NZ3/02578, awarded to PEF. MS was supported by a grant from the National Science Center, Poland (UMO-2020/39/D/NZ5/02075). The open-access publication has been supported by the Faculty of Biochemistry, Biophysics and Biotechnology under the Strategic Programme Excellence Initiative at Jagiellonian University in Krakow, Poland.

Disclosure

The authors report no conflicts of interest in this work.

References

1. Zhang F, Liu MR, Wan HT. Discussion about several potential drawbacks of PEGylated therapeutic proteins. *Biol Pharm Bull.* 2014;37(3):335–339. doi:10.1248/bpb.b13-00661
2. Costa MB, Picon PD, Sander GB, et al. Pharmacokinetics comparison of two pegylated interferon alfa formulations in healthy volunteers. *BMC Pharmacol Toxicol.* 2018;19(1). doi:10.1186/s40360-017-0192-z
3. Ibrahim M, Ramadan E, Elsadek NE, et al. Polyethylene glycol (PEG): the nature, immunogenicity, and role in the hypersensitivity of PEGylated products. *J Control Release.* 2022;351:215–230. doi:10.1016/J.JCONREL.2022.09.031
4. Deng J, Heybati K, Zhou F. Response to “Safety and effectiveness of SARS-CoV-2 vaccines: a systematic review and meta-analysis. *J Med Virol.* 2021;93(12):6477–6478. doi:10.1002/jmv.27269
5. Ling Y, Zhong J, Luo J. Safety and effectiveness of SARS-CoV-2 vaccines: a systematic review and meta-analysis. *J Med Virol.* 2021;93(12):6486–6495. doi:10.1002/JMV.27203
6. Meo SA, Bukhari IA, Akram J, Meo AS, Klonoff DC. COVID-19 vaccines: comparison of biological, pharmacological characteristics and adverse effects of pfizer/BioNTech and moderna vaccines. *Eur Rev Med Pharmacol Sci.* 2021;25(3):1663–1679. doi:10.26355/EURREV_202102_24877
7. Smyth HF, Carpenter CP, Weil CS. The chronic oral toxicology of the polyethylene glycols. *J Am Pharm Assoc.* 1955;44(1):27–30. doi:10.1002/jps.3030440111
8. Mohamed M, Abu Lila AS, Shimizu T, et al. PEGylated liposomes: immunological responses. *Sci Technol Adv Mater.* 2019;20(1):710–724. doi:10.1080/14686996.2019.1627174
9. Szebeni J, Fülöp T, Dézsi L, Metselaar B, Storm G. Liposomal doxorubicin: the good, the bad and the not-so-ugly. *J Drug Target.* 2016;24(9):765–767. doi:10.3109/1061186X.2016.1172591
10. Szebeni J, Baranyi L, Savay S, et al. Role of complement activation in hypersensitivity reactions to Doxil and HYNIC PEG liposomes: experimental and clinical studies. *J Liposome Res.* 2002;12(1–2):165–172. doi:10.1081/LPR-120004790
11. Szebeni J, Fontana JL, Wassef NM, et al. Hemodynamic changes induced by liposomes and liposome-encapsulated hemoglobin in pigs: a model for pseudoallergic cardiopulmonary reactions to liposomes: role of complement and inhibition by soluble CR1 and anti-C5a antibody. *Circulation.* 1999;99(17):2302–2309. doi:10.1161/01.CIR.99.17.2302
12. Verhoef JFF, Carpenter JF, Anchordoquy TJ, Schellekens H. Potential induction of anti-PEG antibodies and complement activation toward PEGylated therapeutics. *Drug Discov Today.* 2014;19(12):1945–1952. doi:10.1016/j.drudis.2014.08.015
13. Szebeni J, Storm G. Complement activation as a bioequivalence issue relevant to the development of generic liposomes and other nanoparticulate drugs. *Biochem Biophys Res Commun.* 2015;468(3):490–497. doi:10.1016/J.BBRC.2015.06.177

14. Ansari L, Shiehzhadeh F, Taherzadeh Z, et al. The most prevalent side effects of pegylated liposomal doxorubicin monotherapy in women with metastatic breast cancer: a systematic review of clinical trials. *Cancer Gene Ther.* **2017**;24(5):189–193. doi:10.1038/cgt.2017.9
15. Cheng TL, Chuang KH, Chen BM, Roffler SR. Analytical measurement of pegylated molecules. *Bioconjug Chem.* **2012**;23(5):881–899. doi:10.1021/bc200478w
16. Fu J, Wu E, Li G, Wang B, Zhan C. Anti-PEG antibodies: current situation and countermeasures. *Nano Today.* **2024**;55:102163. doi:10.1016/J.NANTOD.2024.102163
17. Richter AW, Åkerblom E. Antibodies against polyethylene glycol produced in animals by immunization with monomethoxy polyethylene glycol modified proteins. *Int Arch Allergy Immunol.* **1983**;70(2):124–131. doi:10.1159/000233309
18. Polack FP, Thomas SJ, Kitchin N, et al. Safety and efficacy of the BNT162b2 mRNA Covid-19 vaccine. *N Engl J Med.* **2020**;383(27):2603–2615. doi:10.1056/nejmoa2034577
19. Hossaini S, Keramat F, Cheraghi Z, Zareie B, Doosti-Irani A. Comparing the efficacy and adverse events of available COVID-19 vaccines through randomized controlled trials: updated systematic review and network meta-analysis. *J Res Health Sci.* **2023**;23(4):e00593. doi:10.34172/jrhs.2023.128
20. Shimabukuro T, Nair N. Allergic reactions including anaphylaxis after receipt of the first dose of Pfizer-BioNTech COVID-19 vaccine. *JAMA.* **2021**;325(8):780–781. doi:10.1001/JAMA.2021.0600
21. Zhang P, Sun F, Liu S, Jiang S. Anti-PEG antibodies in the clinic: current issues and beyond PEGylation. *J Control Release.* **2016**;244:184–193. doi:10.1016/j.jconrel.2016.06.040
22. Yang Q, Jacobs TM, McCallen JD, et al. Analysis of pre-existing IgG and IgM antibodies against polyethylene glycol (PEG) in the general population. *Anal Chem.* **2016**;88(23):11804–11812. doi:10.1021/acs.analchem.6b03437
23. Karabasz A, Szczepanowicz K, Cierniak A, et al. In vivo studies on pharmacokinetics, toxicity and immunogenicity of polyelectrolyte nanocapsules functionalized with two different polymers: poly-L-glutamic acid or PEG. *Int J Nanomed.* **2019**;14:9587–9602. doi:10.2147/IJN.S230865
24. Wang GG, Calvo KR, Pasillas MP, Sykes DB, Häcker H, Kamps MP. Quantitative production of macrophages or neutrophils ex vivo using conditional Hoxb8. *Nature Methods.* **2006**;3(4):287–293. doi:10.1038/nmeth865
25. Karabasz A, Bzowska M, Bereta J, Czarnek M, Sochalska M, Klaus T. Mouse IgG3 binding to macrophage-like cells is prevented by deglycosylation of the antibody or by Accutase treatment of the cells. *Sci Rep.* **2021**;11(1). doi:10.1038/s41598-021-89705-3
26. Celis J. *Cell Biology: A Laboratory Handbook*. 2nd ed. Elsevier; **1998**.
27. Schindelin J, Arganda-Carreras I, Frise E, et al. Fiji: an open-source platform for biological-image analysis. *Nature Methods.* **2012**;9(7):676–682. doi:10.1038/nmeth.2019
28. Ershov D, Phan MS, Pylvänäinen JW, et al. TrackMate 7: integrating state-of-the-art segmentation algorithms into tracking pipelines. *Nature Methods.* **2022**;19(7):829–832. doi:10.1038/s41592-022-01507-1
29. Moghimi SM, Szebeni J. Stealth liposomes and long circulating nanoparticles: critical issues in pharmacokinetics, opsonization and protein-binding properties. *Prog Lipid Res.* **2003**;42(6):463–478. doi:10.1016/S0163-7827(03)00033-X
30. Schoenbrunn A, Juelke K, Reipert BM, Horling F, Turecek PL. Polyethylene glycol 20 kDa-induced vacuolation does not impair phagocytic function of human monocyte-derived macrophages. *Front Immunol.* **2022**;13:894411. doi:10.3389/FIMMU.2022.894411/BIBTEX
31. Fang JL, Vanlandingham MM, Beland FA, et al. Toxicity of high-molecular-weight polyethylene glycols in Sprague Dawley rats. *Toxicol Lett.* **2022**;359:22–30. doi:10.1016/J.TOXLET.2022.01.011
32. Caliceti P, Veronese FM. Pharmacokinetic and biodistribution properties of poly(ethylene glycol)–protein conjugates. *Adv Drug Deliv Rev.* **2003**;55(10):1261–1277. doi:10.1016/S0169-409X(03)00108-X
33. Longley CB, Zhao H, Lozanguiez YL, Conover CD. Biodistribution and excretion of radiolabeled 40 kDa polyethylene glycol following intravenous administration in mice. *J Pharm Sci.* **2013**;102(7):2362–2370. doi:10.1002/JPS.23506
34. Bedard K, Krause KH. The NOX family of ROS-generating NADPH oxidases: physiology and pathophysiology. *Physiol Rev.* **2007**;87(1):245–313. doi:10.1152/PHYSREV.00044.2005
35. Ray PD, Huang BW, Tsuji Y. Reactive oxygen species (ROS) homeostasis and redox regulation in cellular signaling. *Cell Signal.* **2012**;24(5):981–990. doi:10.1016/J.CELLSIG.2012.01.008
36. Yang J, Xu L, Di L, Su Y, Zhu X. Journey of Poly(ethylene Glycol) in living cells. *ACS Appl Mater Interfaces.* **2021**;13(34):40267–40277. doi:10.1021/ACSAMI.1C09366/ASSET/IMAGES/LARGE/AMIC09366_0010.JPEG
37. Ulbricht J, Jordan R, Luxenhofer R. On the biodegradability of polyethylene glycol, polypeptides and poly(2-oxazoline)s. *Biomaterials.* **2014**;35(17):4848–4861. doi:10.1016/J.BIOMATERIALS.2014.02.029
38. Sung HJ, Chandra P, Treiser MD, et al. Synthetic polymeric substrates as potent pro-oxidant versus anti-oxidant regulators of cytoskeletal remodeling and cell apoptosis. *J Cell Physiol.* **2009**;218(3):549–557. doi:10.1002/JCP.21629
39. Zemlianskikh NG, Babiychuk LA. The production of reactive oxygen species in human erythrocytes during cryopreservation with glycerol and polyethylene glycol. *Biophysics.* **2019**;4(64):560–567. doi:10.1134/S0006350919040237
40. Liu-Snyder P, Logan MP, Shi R, Smith DT, Borgens RB. Neuroprotection from secondary injury by polyethylene glycol requires its internalization. *J Exp Biol.* **2007**;210(8):1455–1462. doi:10.1242/JEB.02756
41. Sonderegger I, Iezzi G, Maier R, Schmitz N, Kurrer M, Kopf M. GM-CSF mediates autoimmunity by enhancing IL-6-dependent Th17 cell development and survival. *J Exp Med.* **2008**;205(10):2281–2294. doi:10.1084/jem.20071119
42. Liu Z, Li W, Wang F, et al. Enhancement of lipopolysaccharide-induced nitric oxide and interleukin-6 production by PEGylated gold nanoparticles in RAW264.7 cells. *Nanoscale.* **2012**;4(22):7135–7142. doi:10.1039/C2NR31355C
43. Chang CJ, Chen CH, Chen BM, et al. A genome-wide association study identifies a novel susceptibility locus for the immunogenicity of polyethylene glycol. *Nat Commun.* **2017**;8(1):1–7. doi:10.1038/s41467-017-00622-4
44. Amer LD, Saleh LS, Walker C, et al. Inflammation via myeloid differentiation primary response gene 88 (MyD88) signaling mediates the fibrotic response to implantable synthetic poly(ethylene glycol) hydrogels. *Acta Biomater.* **2019**;100:105. doi:10.1016/J.ACTBIO.2019.09.043
45. Napolitani G, Rinaldi A, Bertoni F, Sallusto F, Lanzavecchia A. Selected Toll-like receptor agonist combinations synergistically trigger a T helper type 1-polarizing program in dendritic cells. *Nat Immunol.* **2005**;6(8):769–776. doi:10.1038/ni1223
46. Kaisho T, Akira S. Regulation of dendritic cell function through toll-like receptors. *Curr Mol Med.* **2005**;3(4):373–385. doi:10.2174/1566524033479726

47. Wang Y, Deng W, Lee DY, et al. Age-associated disparity in phagocytic clearance affects the efficacy of cancer nanotherapeutics. *Nat Nanotechnol.* 2023;19(2):255–263. doi:10.1038/S41565-023-01502-3
48. Asoudeh M, Nguyen N, Raith M, et al. PEGylated nanoparticles interact with macrophages independently of immune response factors and trigger a non-phagocytic, low-inflammatory response. *J Control Release.* 2024;366:282–296. doi:10.1016/J.JCONREL.2023.12.019
49. Kenny EF, Herzig A, Krüger R, et al. Diverse stimuli engage different neutrophil extracellular trap pathways. *Elife.* 2017;6:e24437. doi:10.7554/ELIFE.24437
50. Pandurangan M, Veerappan M, Kim DH. Cytotoxicity of zinc oxide nanoparticles on antioxidant enzyme activities and mRNA expression in the cocultured C2C12 and 3T3-L1 cells. *Appl Biochem Biotechnol.* 2015;175(3):1270–1280. doi:10.1007/S12010-014-1351-Y/FIGURES/11
51. Yang EJ, Kim S, Kim JS, Choi IH. Inflammasome formation and IL-1 β release by human blood monocytes in response to silver nanoparticles. *Biomaterials.* 2012;33(28):6858–6867. doi:10.1016/J.BIOMATERIALS.2012.06.016
52. de Bont CM, Koopman WJH, Boelens WC, Puijn GJM. Stimulus-dependent chromatin dynamics, citrullination, calcium signalling and ROS production during NET formation. *Biochim Biophys Acta Mol Cell Res.* 2018;1865(11):1621–1629. doi:10.1016/J.BBAMCR.2018.08.014
53. Lu YJ, Wang YH, Sahu RS, et al. Mechanism of nanoformulated graphene oxide-mediated human neutrophil activation. *ACS Appl Mater Interfaces.* 2020;12(36):40141–40152. doi:10.1021/ACSAMI.0C12490/ASSET/IMAGES/LARGE/AM0C12490_0008.JPEG
54. Melero I, Villalba-Esparza M, Recalde-Zamacona B, et al. Neutrophil extracellular traps, local IL-8 expression, and cytotoxic T-Lymphocyte response in the lungs of patients with fatal COVID-19. *Chest.* 2022;162(5):1006–1016. doi:10.1016/J.CHEST.2022.06.007
55. Shu Q, Zhang N, Liu Y, et al. IL-8 triggers neutrophil extracellular trap formation through an nicotinamide adenine dinucleotide phosphate oxidase- and mitogen-activated protein kinase pathway-dependent mechanism in uveitis. *Invest Ophthalmol Vis Sci.* 2023;64(13). doi:10.1167/IOVS.64.13.19
56. Hann J, Bueb JL, Tolle F, Bréhard S. Calcium signaling and regulation of neutrophil functions: still a long way to go. *J Leukoc Biol.* 2020;107(2):285–297. doi:10.1002/JLB.3RU0719-241R
57. Son S, Yoon SH, Chae BJ, et al. Neutrophils facilitate prolonged inflammasome response in the DAMP-rich inflammatory milieu. *Front Immunol.* 2021;12:746032. doi:10.3389/FIMMU.2021.746032/BIBTEX
58. Ng LG, Ostuni R, Hidalgo A. Heterogeneity of neutrophils. *Nat Rev Immunol.* 2019;19(4):255–265. doi:10.1038/s41577-019-0141-8
59. Clemens RA, Chong J, Grimes D, Hu Y, Lowell CA. STIM1 and STIM2 cooperatively regulate mouse neutrophil store-operated calcium entry and cytokine production. *Blood.* 2017;130(13):1565–1577. doi:10.1182/BLOOD-2016-11-751230
60. Parker H, Dragunow M, Hampton MB, Kettle AJ, Winterbourn CC. Requirements for NADPH oxidase and myeloperoxidase in neutrophil extracellular trap formation differ depending on the stimulus. *J Leukoc Biol.* 2012;92(4):841–849. doi:10.1189/JLB.1211601
61. Gupta AK, Giaglis S, Hasler P, Hahn S. Efficient neutrophil extracellular trap induction requires mobilization of both intracellular and extracellular calcium pools and is modulated by cyclosporine A. *PLoS One.* 2014;9(5):e97088. doi:10.1371/JOURNAL.PONE.0097088
62. Kucherenko Y, Bernhardt I. The study of Ca²⁺ influx in human erythrocytes in isotonic polyethylene (glycol) 1500 (PEG-1500) and sucrose media. *Ukr Biokhim Zh.* 2006;78:46–52.
63. Krémer V, Godon O, Bruhns P, Jönsson F, de Chaisemartin L. Isolation methods determine human neutrophil responses after stimulation. *Front Immunol.* 2023;14. doi:10.3389/FIMMU.2023.1301183
64. McSweeney MD, Shen L, DeWalle AC, et al. Pre-treatment with high molecular weight free PEG effectively suppresses anti-PEG antibody induction by PEG-liposomes in mice. *J Control Release.* 2021;329:774–781. doi:10.1016/J.JCONREL.2020.10.011

International Journal of Nanomedicine

Dovepress

Publish your work in this journal

The International Journal of Nanomedicine is an international, peer-reviewed journal focusing on the application of nanotechnology in diagnostics, therapeutics, and drug delivery systems throughout the biomedical field. This journal is indexed on PubMed Central, MedLine, CAS, SciSearch®, Current Contents®/Clinical Medicine, Journal Citation Reports/Science Edition, EMBase, Scopus and the Elsevier Bibliographic databases. The manuscript management system is completely online and includes a very quick and fair peer-review system, which is all easy to use. Visit <http://www.dovepress.com/testimonials.php> to read real quotes from published authors.

Submit your manuscript here: <https://www.dovepress.com/international-journal-of-nanomedicine-journal>